SEMARAK ILMU
PUBLISHING

Journal of Advanced Research in Applied Sciences and Engineering Technology

Journal homepage:
https://semarakilmu.com.my/journals/index.php/araset
ISSN: 2462-1943

Thermomechanical Optimization of Drill Margin Geometry in Drilling of Ti-6Al-4V: A Coupled FEM-RSM Investigation

Taher Sherif Fathi Mohamed Hassan[1], Mohd Faizal Ali Akhbar [1,*]

[1] Department of Maritime Technology and Naval Architecture, Faculty of Ocean Engineering Technology, Universiti Malaysia Terengganu, 21030 Kuala Nerus, Terengganu, Malaysia

ARTICLE INFO

Article history:
Received 21 April 2026
Received in revised form 14 June 2026
Accepted 15 June 2026
Available online 18 June 2026

Keywords:
Titanium; Drilling; Ti-6Al-4V; Response Surface Methodology

ABSTRACT

Drilling of titanium alloys generates extreme temperatures, cutting forces, and torque due to their poor thermal conductivity and strong tool–workpiece interaction. These extreme thermomechanical outputs could shorten drill span, reduce hole quality, and increase costs. The drill margin dimensions control frictional contact between the tool and the hole wall. However, the influence of drill margin on thermo-mechanical responses has been scarcely investigated in titanium drilling. In this study, a thermomechanical finite element model (FEM) was developed to analyze the effects of drill margin width (M_w) and margin height (M_h) on drilling temperature, thrust force, and torque. A face-centered central composite design was employed to evaluate the influence of the margin parameters. Response surface methodology (RSM) was used to develop predictive models of temperature, thrust force, and torque. The developed FEM was validated against the experimental results of Chatterjee et al. (2016) at various rotational speeds and feeds in the ranges of 400-600 rev/min and 30-50 mm/min, respectively. The force results produced an average prediction error of 2.5 %, which indicates the simulation model is sufficiently accurate to predict the drilling outputs. The results revealed that both M_w and M_h significantly influence drilling performance by varying the frictional contact between the drill margin and the hole wall. Increasing the margin dimensions increases temperature, thrust force, and torque due to intensified rubbing contact. Response surface analysis unveiled a strong interaction between M_w and M_h. The optimal configuration within the investigated design space was identified at M_w = 9% and M_h = 2%. The findings provide useful insights for optimizing drill margin geometry to improve drilling efficiency in titanium alloy (Ti-6Al-4V) machining.

1. Introduction

Titanium (Ti-6Al-4V) is widely used across aerospace, biomedical, and manufacturing industries because of its excellent strength-to-weight ratio (1265 MPa tensile strength at a density of 4.43 g/cm3 [1]), corrosion resistance [2], and biocompatibility [3]. However, its machinability index is among the lowest of structural alloys, which is approximately 22% relative to free-cutting steel [4]. The reasons are because of its low thermal conductivity (6.7 W/m·K [4]), its strong chemical affinity

* *Corresponding author.*
E-mail address: mfaizalaa@umt.edu.my

https://doi.org/10.37934/araset.40.5.446466

for cutting tool materials, and its retention of hardness at elevated temperatures [5]. During drilling, these characteristics produce concentrated heat at the tool–workpiece interface. For example, temperatures of 450-540 °C have been recorded at the drill tip during dry drilling of Ti-6Al-4V, compared with approximately 210-340 °C for aluminum alloys under similar cutting conditions [6]. Consequently, tool wear rates in titanium drilling are substantially higher than in steels. The associated increase in thrust force and torque further degrades hole dimensional accuracy and surface integrity, both of which are safety-critical in aerospace and orthopedic applications [7]. Therefore, controlling thermal and mechanical loads during drilling is critical to improving tool life and machining efficiency.

Among the geometric features of twist drills, the drill margin stabilizes the tool during drilling and maintains hole dimensional accuracy [8]. Margin width (M_w) is the axial thickness of the drill margin to provide stability and guidance of the drill shaft (**Fig. 1**). Margin height (M_h) is the radial protrusion of the margin above the flute surface to maintain contact pressure and friction intensity of the drill shaft against the hole's wall [9, 10]. Drill margin contributes significantly to frictional contact between the drill and the hole surface [11], and excessive margin contact increases friction, resulting in increased temperature, thrust force, and torque during drilling [10]. Therefore, optimizing margin geometry is essential to balance hole stability and frictional heat generation. Previous studies on drilling performance have primarily focused on parameters such as point angle, helix angle, feed rate, and cutting speed [5, 12, 13]. Several researchers have reported that tool geometry significantly influences chip evacuation, cutting forces, and thermal distribution during drilling operations [11, 14, 15]. In particular, modifications to drill geometry have been shown to improve machining performance in difficult-to-cut materials such as titanium alloys. However, despite the importance of the drill margin in controlling tool guidance and frictional interaction with the hole wall, relatively limited attention has been devoted to the influence of margin dimensions on the thermo-mechanical behavior during drilling. Understanding the influence of margin geometry is particularly important in titanium drilling, as the generated heat tends to concentrate near the tool margin and cutting edges due to the material's low thermal diffusivity. This localized heat accumulation can accelerate tool wear and cause thermal damage to the workpiece. Therefore, investigating the relationship between margin geometry and drilling responses such as temperature, thrust force, and torque is essential for improving drilling performance and tool design.

To analyze the complex interactions between geometric parameters and drilling responses, statistical optimization techniques, such as Response Surface Methodology (RSM), have been widely adopted in machining studies [16, 17]. RSM enables the development of predictive models that describe the relationship between input factors and process responses while minimizing the number of experimental runs. In particular, the Central Composite Design (CCD) is commonly used to evaluate quadratic effects and interaction behavior between parameters. When combined with finite element modeling, RSM provides a powerful framework for analyzing thermo-mechanical behavior in machining processes and for identifying optimal parameter combinations. By integrating finite element analysis with statistical modeling techniques such as RSM, it is possible to gain deeper insights into the influence of drill geometry on machining performance [17].

Therefore, the objective of this study is to investigate the influence of drill margin geometry, specifically margin width(M_w) and margin height (M_h), on the thermomechanical performance of titanium drilling. Finite element simulations were conducted to evaluate drilling temperature, thrust force, and torque under different margin configurations. The results were validated with experimental values from Chatterjee et al. (2016) [17]. A face-centered CCD in RSM was employed to develop predictive models and analyze the interaction effects between the factors. The findings of this study provide useful insights into optimizing drill margin design to improve drilling performance in titanium machining.

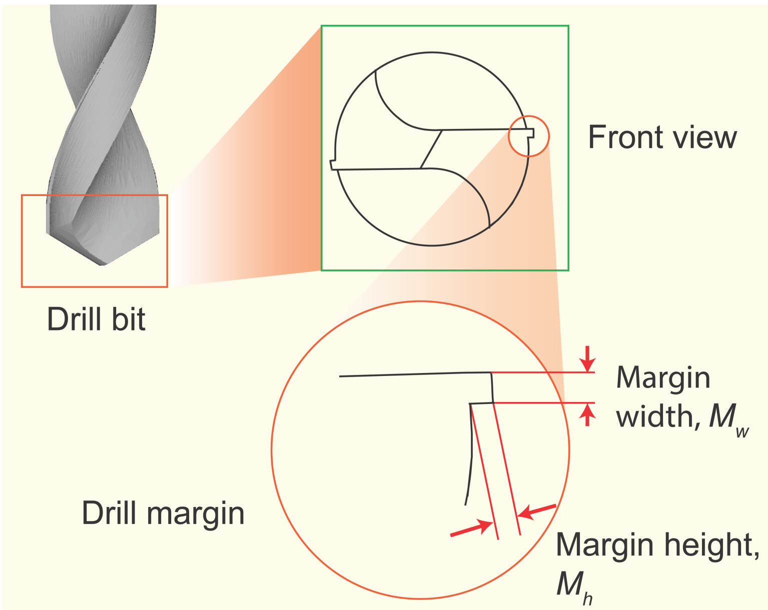

Fig. 1. Anatomy of margin width (M_w) and margin height (M_h).

2. Methodology

2.1 Finite Element Modeling of the Drilling Process

Finite element modeling was performed using the commercial software DEFORM-3D to investigate the thermo-mechanical behavior during drilling of a titanium alloy under different drill margin geometries. The numerical simulations were conducted in a three-dimensional machining simulation environment to capture the temperature distribution, thrust force, and torque generated during drilling.

In the simulation model, the drill was treated as a rigid body, while the workpiece was modeled as a deformable plastic body. This assumption is commonly adopted in machining simulations because the tool material typically has significantly higher stiffness than the workpiece. The workpiece was discretized using adaptive tetrahedral elements to capture large plastic deformation and chip formation during drilling. A refined mesh was applied near the cutting region to improve numerical accuracy in predicting temperature and stress distribution.

The drilling process was simulated under dry cutting conditions. Heat generation during drilling arises primarily from plastic deformation in the shear zone and friction at the tool–workpiece interface. A Coulomb friction model was employed to describe the interaction between the drill surface and the workpiece material. Frictional heat generated at the interface significantly contributes to the overall temperature distribution in the cutting zone.

The governing relationship for frictional heat generation can be expressed as

$$q = \mu F_n v, \tag{1}$$

where q represents the frictional heat generation rate, μ is the friction coefficient, F_n is the normal contact force, and v is the sliding velocity at the tool–workpiece interface. The generated heat was partitioned between the tool and the workpiece based on the materials' thermal properties. The transient heat conduction equation governed temperature evolution within the workpiece

$$\rho c_p \frac{\partial T}{\partial t} = k\nabla^2 T + Q, \tag{2}$$

where ρ is the material density, c_p is the specific heat capacity, k is the thermal conductivity, T represents temperature, and Q denotes internal heat generation due to plastic deformation and friction.

Finite element simulations were performed using DEFORM-3D (v11, SFTC, USA). The workpiece (Ti6Al4V) was modeled as a plastic material with a 65 mm-diameter and 5 mm-thick cylinder [17]. The drill bit, modeled as rigid tungsten carbide [10, 18, 19], had a 5.0 mm diameter, 118° point angle, 30° helix angle, and 18% web thickness [19]. Simple shear friction defined the drill–workpiece interface, expressed as:

$$\tau = m.k, \tag{3}$$

where τ is the frictional shear stress, $m = 0.6$ the friction factor [17], and k the shear yield stress.

Fig. 2 shows the simulation setup for the drilling process. The drill and workpiece models were meshed with 50,000 and 65,000 tetrahedral elements, respectively. Simulations were conducted at 400 rpm, 30 mm/min, and 7 mm drilling depth. Initial temperatures were set to 23°C. The Incremental Lagrangian formulation with a Sparse solver was employed to enhance computational efficiency. Fracture and chip formation in bone was modeled using the Cockroft–Latham criterion:

$$D = \int_0^{\varepsilon_{eff}} \left(\frac{\sigma_{max}}{\sigma_{eff}}\right) d\bar{\varepsilon}, \tag{4}$$

where D denotes the damage accumulation, σ_{max} the maximum stress, and σ_{eff} the effective stress.

The maximum drilling temperature, thrust force, and torque were extracted from the simulation results after the drill reached a steady engagement with the workpiece. These responses were used as performance indicators to evaluate the influence of drill margin geometry on drilling behavior.

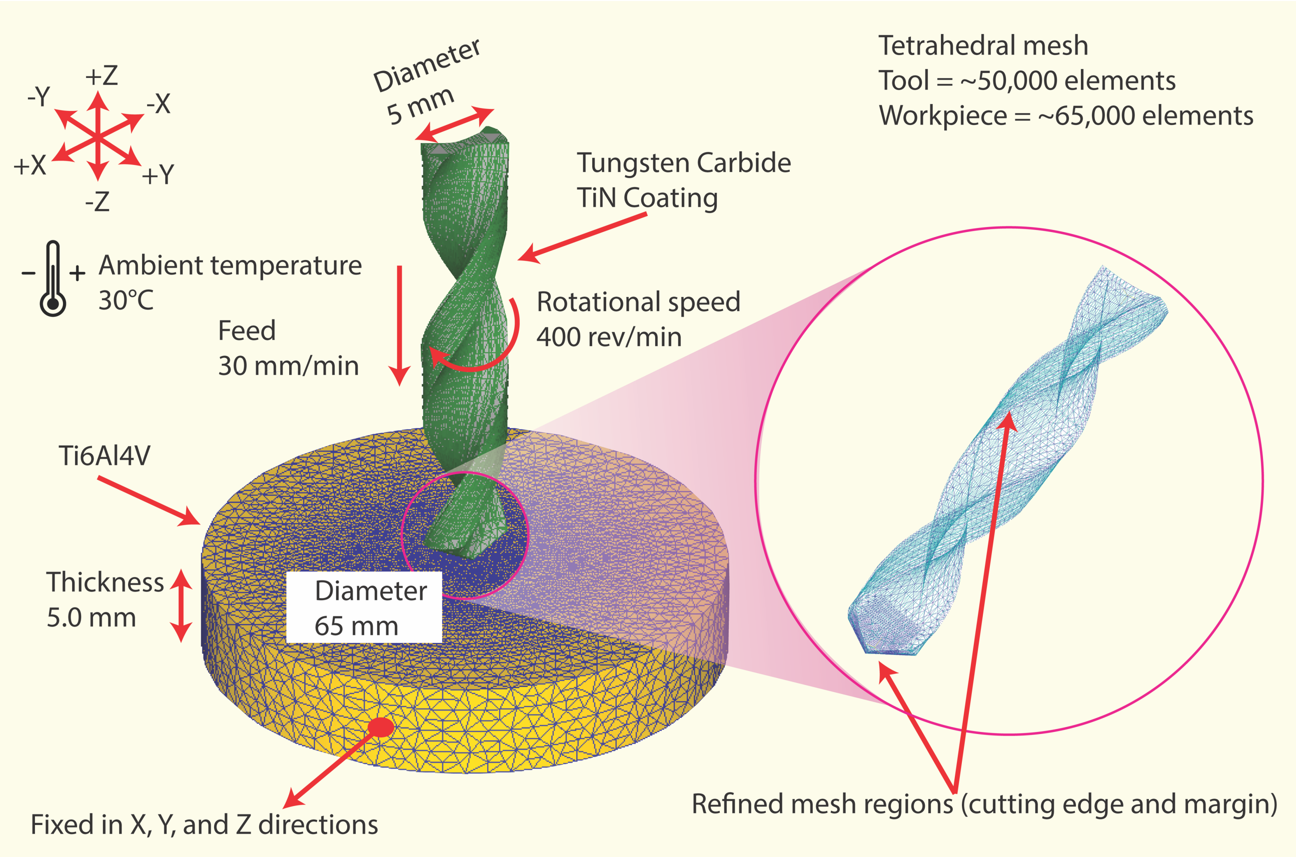

Fig. 2. Drilling simulation setup in DEFORM-3D.

2.2 Validation of Simulation Results

To evaluate the reliability of the developed drilling simulation model, the predicted thrust force and torque were validated against experimental results reported in Chatterjee et al. 2016 [17]. Five representative runs (Run 1, Run 2, Run 3, Run 4, and Run 13) were selected for validation (Table 1). It should be noted that experimental temperature measurements corresponding to the selected validation conditions were not available in the reference study. Consequently, model validation was performed using the available thrust force and torque data. Although force and torque are widely accepted indicators for validating drilling simulations, future work should incorporate direct temperature measurements to further verify the model's thermal predictions.

Table 1
Selected experimental runs from Chatterjee et al. (2016) [17] for validation of simulation results

Run	Rotational speed(rev/ min)	Feed (mm/ min)	Drill diameter (mm)
1	400	30	5
2	600	30	5
3	400	50	5
4	600	50	5
13	500	40	5

2.3 Drill Margin Geometry Parameters

In this study, two geometric parameters describing the drill margin were investigated: (1) margin width (M_w) and (2) margin height (M_h). The selected parameter ranges were determined based on typical drill design guidelines and preliminary simulations to ensure realistic tool geometries [9, 20]. These ranges represent practical variations in drill margin design commonly encountered in industrial drilling tools. The investigated ranges are summarized in Table 2.

Table 2
Factors and levels used in the Response Surface Methodology (RSM) study.

Factor	Level -1	Level 0	Level +1
Margin Width, M_w (%)	9	9.5	10
Margin Height, M_h (%)	2	3	4

2.4 Experimental Design Using Response Surface Methodology (RSM)

To systematically evaluate the influence of margin geometry on drilling performance, Response Surface Methodology (RSM) was employed using Design Expert software (Version 13, Stat-Ease Inc., Minneapolis, MN). RSM is a statistical technique used to develop empirical models that describe the relationship between input factors and process responses while reducing the number of required experiments or simulations [9, 15, 19]. A face-centered central composite design (CCD) was adopted in this study to investigate the effects of margin width and margin height on drilling responses. The CCD design consists of factorial points, axial points, and replicated center points, allowing estimation of linear, quadratic, and interaction effects among the factors [9].

The design consisted of four factorial points, four axial points, and one center point, resulting in a total of nine simulation runs. Since the responses were obtained from deterministic finite element simulations, replication of center points was not required. A second-order polynomial model was used to represent the relationship between the input factors and the drilling responses. The general form of the regression model is given by

$$Y = \beta_0 + \sum_i^k \beta_i X_i + \sum_{i=1}^{k-1} \sum_{j=i+1}^{k} \beta_{ij} X_i X_j + \sum_{i=1}^{k} \left(\beta_{ij} X_i^2 \right) + \varepsilon, \tag{5}$$

where Y is the predicted response(temperature, thrust force, or torque), X_i is the input variable, β are coefficients, and ε is the residual error.

Analysis of variance (ANOVA) was performed to evaluate the statistical significance of the developed models and to identify the dominant factors influencing drilling performance. Contour and three-dimensional response surface plots were subsequently generated to visualize the interaction effects among the geometric parameters.

2.5 Optimization of Drill Margin Geometry

The developed response surface models were used to identify the optimal margin geometry that simultaneously minimizes drilling temperature, thrust force, and torque. Multi-response optimization was conducted using a desirability-based approach, where each response was transformed into a desirability function ranging from 0 to 1 [9, 21]. The optimal solution corresponds to the factor combination that maximizes the overall desirability. The optimized margin geometry provides practical guidelines for improving drilling performance and reducing thermal loading during machining of titanium alloys.

The desirability function approach was adopted for multi-response optimization due to its ease of application and versatility [15, 21]. This technique standardizes all responses onto a scale from 0 to 1, where 1 signifies the optimal response and 0 denotes an undesirable result. All target responses were assessed collectively to identify an optimal trade-off solution. The optimization was conducted using five options for setting response goals: none, maximize, minimize, within range, and target. The corresponding mathematical expressions for these functions are provided in Eqs. (6)–(9):

- maximum objective functions,

$$d_i = 0, Y_i < Low_i \tag{6}$$
$$d_i = \left[\frac{Y_i - Low_i}{T_i - Low_i}\right], Low_i \le T_i \le Y_i$$
$$d_i = 1, Y_i > T_i$$

- minimum objective functions,

$$d_i = 1, Y_i < T_i \tag{7}$$
$$d_i = \left[\frac{Y_i - High_i}{T_i - High_i}\right], T_i \le Y_i \le High_i$$
$$d_i = 0, Y_i > High_i$$

- within-range objective functions,

$$d_i = 0, Y_i \le Low_i \tag{8}$$
$$d_i = 1, Low_i < Y_i < High_i$$
$$d_i = 0, Y_i \ge High_i$$

- target objective functions:

$$d_i = 0, Y_i < Low_i \tag{9}$$
$$d_i = \left[\frac{Y_i - Low_i}{T_i - Low_i}\right]^{wt_i}, Low_i \le T_i \le Y_i$$
$$d_i = \left[\frac{Y_i - High_i}{T_i - High_i}\right]^{wt_i}, T_i \le Y_i \le High_i$$
$$d_i = 0, Y_i > High_i d_i = 0, Y_i > High_i$$

where d_i, Y_i, Low_i, $High_i$, T_i, and wt_i denote the individual desirability, response variable, lower acceptable values, upper acceptable values, and weight assigned to the target value, respectively.

3. Results and Discussion

3.1 Validation of Simulation Models

Fig. 3 compares the experimental measurements reported in the literature [17] with the predictions from the present FEM simulations. The results demonstrate good agreement between the FEM predictions and the experimental measurements. The relative error for thrust force ranges from 0.73% to 4.89%, with an average deviation of approximately 2.5%. These small deviations indicate that the developed numerical model captures the mechanical behavior of the drilling process. The obtained prediction accuracy, with an average error of approximately 2.5%, demonstrates that the developed FEM model provides reliable predictions of drilling forces and can therefore be confidently used for parametric analysis and optimization of drill margin geometry.

The close agreement between the numerical predictions and the experimental results confirms the developed finite element model's ability to accurately simulate drilling forces and torque. The minor deviations observed between the simulated and experimental results may be attributed to simplifications in the friction model, uncertainties in the material constitutive behavior, and variations in experimental conditions. Nevertheless, the obtained prediction accuracy is comparable to or better than that reported in previous drilling simulation studies, including simulation modeling of drilling performance using FEM and RSM. Therefore, the validated finite element model can be considered reliable for investigating the influence of drill margin geometry on drilling temperature, thrust force, and torque.

Despite the good agreement between the numerical and experimental results, several assumptions and simplifications were adopted in the present finite element model. The Ti-6Al-4V workpiece was assumed to be homogeneous and isotropic, whereas actual materials may exhibit local microstructural variations that influence deformation and heat generation. The drill was modeled as a rigid body, and progressive tool wear was not considered during the simulations. Furthermore, all simulations were performed under dry drilling conditions, and the effects of coolant application, minimum quantity lubrication (MQL), or cryogenic cooling were not included. The friction coefficient was assumed to remain constant throughout the drilling process, although friction conditions may vary with temperature, tool wear, and chip accumulation in practical machining operations. Consequently, the model may not fully capture all physical phenomena occurring during industrial drilling. Nevertheless, the average prediction error of approximately 2.5% observed during validation indicates that the model is sufficiently accurate to evaluate the relative influence of drill margin geometry on temperature, thrust force, and torque within the investigated parameter range.

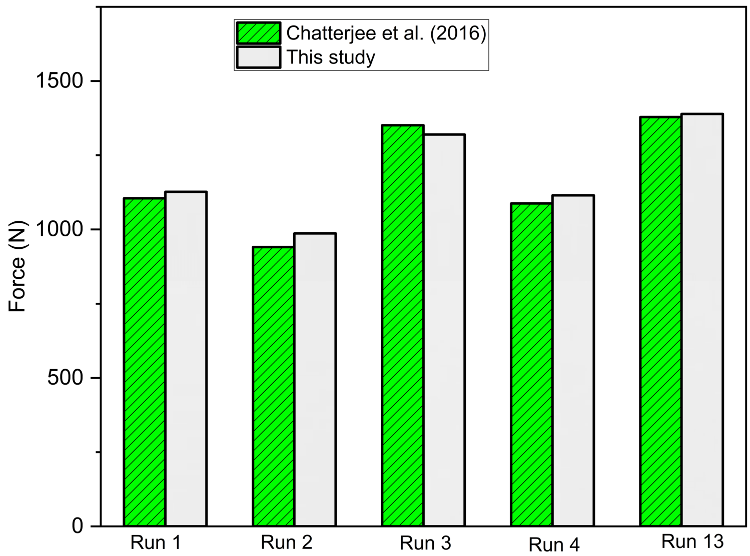

Fig. 3. Validation of simulation results (force) with the experimental results of Chatterjee et al. (2016) [17].

3.2 ANOVA of Thermomechanical Outputs

The thermomechanical outputs from the RSM, coupled with the simulation study, are presented in **Table 3**. These results were analyzed using ANOVA to determine the best model to represent the data.

Table 3
Results for temperature, force, and torque from the simulation study.

Run	Margin height, M_h (%)	Margin width, M_w (%)	Temperature (°C)	Force (N)	Torque (Nmm)
1	9	3	385.1	879.8	4949.7
2	9	2	355.3	820.4	469.8
3	10	4	455.4	1280.2	5450.4
4	9.5	3	400.2	905.1	5100.2
5	9	4	430.4	1080.1	5200.2
6	9.5	2	372.3	860.3	4850.7
7	10	2	382.1	890.3	4900.3
8	10	3	412.1	960.2	5150.2
9	9.5	4	438.3	1150.1	5349.8

3.21 ANOVA of Temperature

The linear model for temperature fit the data well, with R^2 = 0.9881, Adjusted R^2 = 0.9841, and Predicted R^2 = 0.9735 (difference < 0.2). The small differences between these values confirm that the generalization is reliable without overfitting (**Table 4**). The Model F-value of 248.45 ($p < 0.0001$) confirms overall significance, with all main effects (M_w and M_h). Between these factors, M_w contributes to the highest F-value (437.31. These results show that it is the dominant factor affecting the temperature. The reason could be increased radial contact between the drill margin and the hole wall, which enhances frictional heat generation during drilling. In contrast, margin width has a comparatively smaller but still significant effect on the temperature. Model adequacy was further supported by an Adequate Precision of 40.49, which is above the threshold of 4.0. This value indicates strong signal-to-noise discrimination across the design space. The resulting regression equation (Eq. 6) is used to map the T_{max} response surface and identify thermally favorable margin configurations.

$$T_{max} = 403.22 + 13.17A + 35.67B, \tag{10}$$

Table 4
ANOVA results for maximum temperature, T_{max}.

Source	Sum of Squares	df	Mean Square	F-value	p-value	Remarks
Model	8672.83	2	4336.42	248.45	< 0.0001	Significant
A-M_w	1040.17	1	1040.17	59.59	0.0002	Significant
B-M_h	7632.67	1	7632.67	437.31	< 0.0001	Significant
Residual	104.72	6	17.45			
Cor Total	8777.55	8				
Std. Dev.	4.18		R^2	0.9881		
Mean	403.22		Adjusted R^2	0.9841		
C.V. %	1.04		Predicted R^2	0.9735		
			Adeq Precision	40.49		

3.22 ANOVA of Force

The results indicate that the model is statistically significant, with an F-value of 80.99 and a p-value of 0.0021, confirming that the model adequately describes the relationship between the input parameters and the response. Both margin width (MW) and margin height (MH) had significant effects on thrust force, with p-values of 0.0072 and 0.0004, respectively. Among the two factors, margin height exhibits a substantially higher F-value (311.25) compared to margin width (43.15), indicating that MH is the dominant parameter influencing thrust force. This behavior can be attributed to increased radial contact and frictional resistance between the drill margin and the hole wall as the margin height increases. The interaction between M_w and M_h is marginally significant (p = 0.0582), suggesting a relatively weak interaction between the two parameters. In contrast, the quadratic term of margin height (M_h^2) is statistically significant (p = 0.0078), indicating the presence of a nonlinear relationship between margin height and thrust force. However, the quadratic term for margin width (M_w^2) was found to be insignificant.

The model exhibits excellent statistical performance, with a coefficient of determination (R^2) of 0.9926, indicating that more than 99% of the variation in thrust force is explained by the model. The adjusted R^2 (0.9804) and predicted R^2 (0.9104) are in good agreement. This accord confirms the model's robustness and predictive capability. Furthermore, the low coefficient of variation (2.22%) and high adequate precision (21.21) indicate high reliability and a strong signal-to-noise ratio.

Table 5
ANOVA results for force.

Source	Sum of Squares	df	Mean Square	F-value	p-value	Remarks
Model	191600.00	5	38320.56	80.99	0.0021	Significant
A-M_w	20416.67	1	20416.67	43.15	0.0072	Significant
B-M_h	147300.00	1	147300.00	311.25	0.0004	Significant
AB	4225.00	1	4225.00	8.93	0.0582	
A^2	355.56	1	355.56	0.7515	0.4498	
B^2	19338.89	1	193338.89	40.87	0.0078	Significant
Residual	1419.44	3	473.15			
Cor Total	193000	8				
Std. Dev.	21.75		R^2	0.9926		
Mean	980.56		Adjusted R^2	0.9804		
C.V. %	2.22		Predicted R^2	0.9104		
			Adeq Precision	21.21		

3.23 ANOVA of Torque

Analysis of variance (ANOVA) was performed to evaluate the statistical significance of the developed regression model for drilling torque. The results indicate that the model is highly significant, with an F-value of 586.37 and a p-value of 0.0001. These characteristics confirm the model's adequacy in representing the relationship between the input parameters (M_w and M_h) and the responses (torque). Both M_w and M_h were found to significantly influence torque, with p-values of 0.0002 and less than 0.0001, respectively. Among these factors, margin height shows a substantially higher F-value (2471.14) than margin width (434.57). This significant difference indicates that M_h is the dominant parameter affecting torque. This behavior is attributed to increased frictional resistance at the tool–workpiece interface as the margin height increases. The interaction effect between M_w and M_h was found to be statistically insignificant (p = 0.1443), which suggests that the influence of the two parameters on torque is independent. Regarding the quadratic terms, the square of margin width (M_w^2) is significant (p = 0.0190), which shows a nonlinear relationship between M_w and torque, whereas the quadratic term of margin height (M_h^2) is insignificant.

The developed model demonstrates excellent statistical performance, with a coefficient of determination (R^2) of 0.9990. This trend indicates that nearly all the torque variability is explained by the model. The adjusted R^2 (0.9973) and predicted R^2 (0.9882) are in close agreement, which confirms the robustness and predictive capability of the model. Additionally, the very low coefficient of variation (0.25%) and high adequate precision (70.56) indicate excellent model reliability and a strong signal-to-noise ratio.

Table 6
ANOVA results for torque

Source	Sum of Squares	df	Mean Square	F-value	p-value	Remarks
Model	475100.00	5	95013.89	586.37	0.0001	Significant
A-M_w	70416.67	1	70416.67	434.57	0.0002	Significant
B-M_h	400400.00	1	4.004E+05	2471.14	< 0.0001	Significant
AB	625.00	1	625.00	3.86	0.1443	
A^2	3472.22	1	3472.22	21.43	0.0190	Significant
B^2	138.89	1	138.89	0.8571	0.4228	
Residual	486.11	3	162.04			
Cor Total	475600.00	8				
Std. Dev.	12.73		R^2	0.9990		
Mean	5072.22		Adjusted R^2	0.9973		
C.V. %	0.2510		Predicted R^2	0.9882		
			Adeq Precision	70.5570		

3.3 Diagnostic Analysis of Maximum Temperature, Thrust Force, and Torque
3.31 Diagnostic analysis of Maximum Temperature (T_{max})

Fig. 4 shows the diagnostic results for the linear model of T_{max}. The normal probability plot (**Fig. 4**a) shows that the residuals follow a nearly straight line and are normally distributed. No significant deviation from linearity is observed, and there are no extreme points deviating from the trend line. This trend confirms that the assumption of normality of residuals, which is essential for the validity of ANOVA and regression analysis, is satisfied.

The residuals-versus-predicted values plot shows that the residuals are randomly scattered around the zero line, without any clear systematic pattern (**Fig. 4**b). This pattern indicates that the assumptions of linearity and model adequacy are satisfied. The externally studentized residuals fall within the acceptable limits of ±4.655, and there are no significant outliers in the dataset. Additionally, the spread of residuals appears relatively constant across the range of predicted values.

This characteristic shows the absence of non-constant variance. Overall, this plot confirms that the developed model provides an unbiased prediction of maximum temperature.

The predicted-versus-actual plot shows that the data points lie very close to the 45° reference line and that there is strong agreement between the predicted and actual temperature values (**Fig. 4**c). This trend demonstrates that the regression model has high predictive accuracy, which is consistent with the high coefficient of determination ($R^2 = 0.988$) obtained from the ANOVA analysis in **Table 4**. The small deviations observed are minimal and randomly distributed and therefore confirm the reliability of the model.

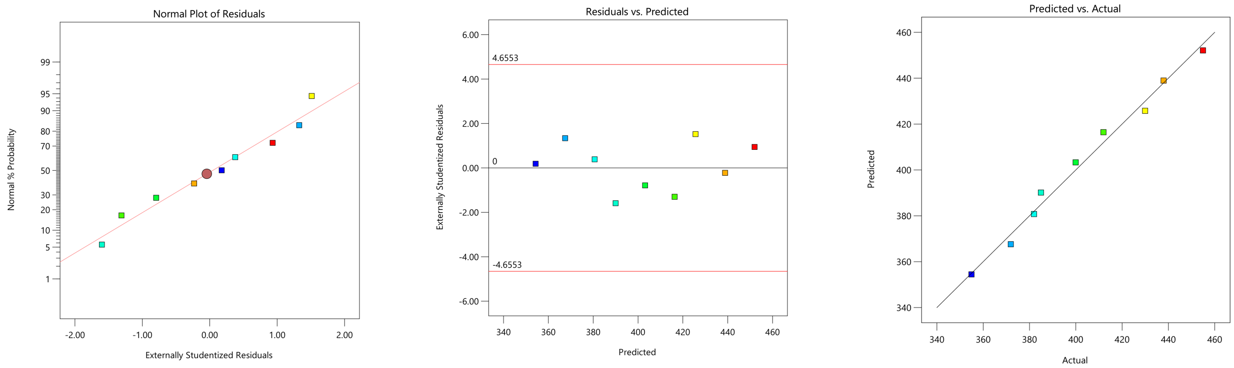

(a) (b) (c)

Fig. 4. Diagnostic assessment of T_{max} consisting of (a) normal plot, (b) residuals vs predicted, and (c) predicted vs actual.

3.31 Diagnostic analysis of Force

Fig. 5 presents the diagnostic results for force. The normal probability plot (**Fig. 5**a) confirms that the errors are normally distributed and therefore supports the adequacy of the least-squares fit. The residuals-versus-predicted plot (**Fig. 5**b) shows no discernible pattern and indicates that the residuals are randomly distributed. Additionally, the predicted versus actual plot (**Fig. 5**c) demonstrates a strong agreement between the predicted and actual values with random patterns. These results confirm that the proposed model is statistically valid, with no violations of independence or of the assumption of constant variance.

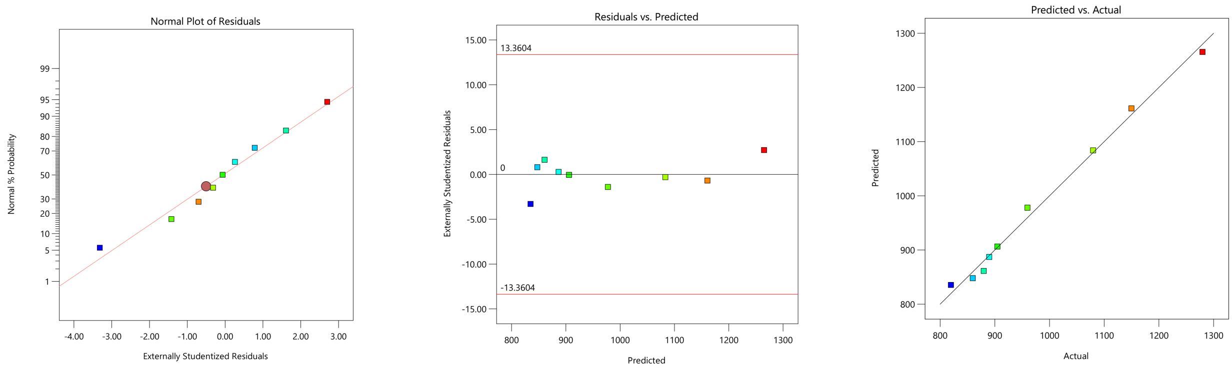

(a) (b) (c)

Fig. 5. Diagnostic assessment of force consisting of (a) normal plot, (b) residuals vs predicted, and (c) predicted vs actual.

3.31 Diagnostic analysis of torque

The diagnostic plots in **Fig. 6** further confirm the adequacy of the developed torque regression model. The normal probability plot demonstrates that the residuals follow an approximately normal distribution (**Fig. 6**a). The residuals are randomly distributed without any noticeable pattern, and therefore reveal that the assumptions of linearity and constant variance are satisfied (**Fig. 6**b). Furthermore, the predicted values show excellent agreement with the actual data, as evidenced by their close alignment along the 45° line (**Fig. 6**c). These results confirm that the developed model is statistically reliable and can be effectively used for prediction and optimization of drilling torque.

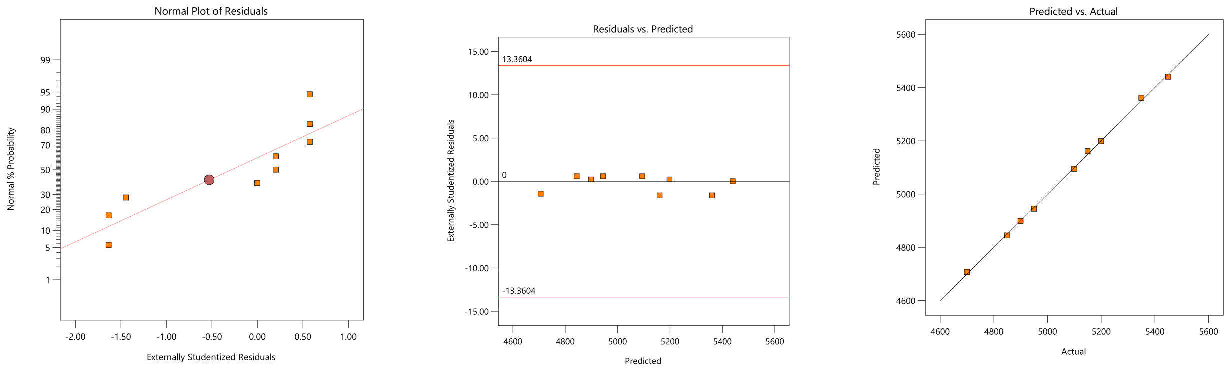

(a) (b) (c)

Fig. 6. Diagnostic assessment of torque consisting of (a) normal plot, (b) residuals vs predicted, and (c) predicted vs actual.

3.4 Surface Plots and Parameters Interactions

The three-dimensional response surface and contour plots were used to investigate the combined effects of margin width (M_w) and margin height (M_h) on drilling temperature, thrust force, and torque. These plots provide a clear visualization of the interaction between the input parameters and their influence on the drilling responses.

3.41 Surface Plots of Maximum Temperature (T_{max})

The one-factor effect plots and contours for maximum temperature are shown in **Fig. 7**. The trends in **Fig. 7**a and 7b show clear increases with both M_w and M_h. However, the surface exhibits a steeper gradient along the M_h. This trend indicates that M_h produces a stronger influence on temperature than M_w. At higher values of M_h, the temperature increases significantly due to greater radial contact between the drill margin and the hole wall, which enhances frictional heating. In contrast, the influence of M_w is relatively moderate, contributing mainly through an increase in the contact area. The contour plot further confirms this behavior, with closely spaced contour lines along the M_h direction, which reveals a rapid increase in temperature with increasing margin height (**Fig. 7**c). This observation is consistent with the ANOVA results, which show that M_h (437.13) had a significantly higher F-value than M_w (59.59).

The maximum drilling temperatures obtained from the finite element simulations ranged from 355 °C to 455 °C, depending on the margin width and margin height configurations. These values fall within the typical temperature range reported for drilling titanium alloys, confirming the reliability of the simulation results. The influence of margin height on temperature can be clearly observed when the margin width is held constant. For instance, at M_w = 9%, increasing the margin height from 2% to 4% increased the drilling temperature from 355 °C to 430 °C. A similar trend is observed for other margin width levels. This increase can be attributed to the enlargement of the contact area between the drill margin and the hole wall as the margin height increases. The additional contact intensifies frictional interaction, leading to greater heat generation during drilling. A similar effect is observed for margin width. At M_h = 3%, the temperature increased from 385 °C to 412 °C as the margin width increased from 9% to 10%. A wider margin increases the rubbing surface between the drill and the hole wall. This action leads to higher frictional heat generation. Consequently, both the margin width and the margin height play important roles in influencing thermal behavior during drilling.

The combined effect of these parameters indicates an interaction between margin width and margin height. At higher margin heights, the influence of margin width on temperature becomes more significant. For example, when M_h = 4%, the temperature increased from 430 °C to 455 °C as the margin width increased from 9% to 10%. This phenomenon suggests that the combined geometric interaction of the margin dimensions regulates the thermal response of the drilling process.

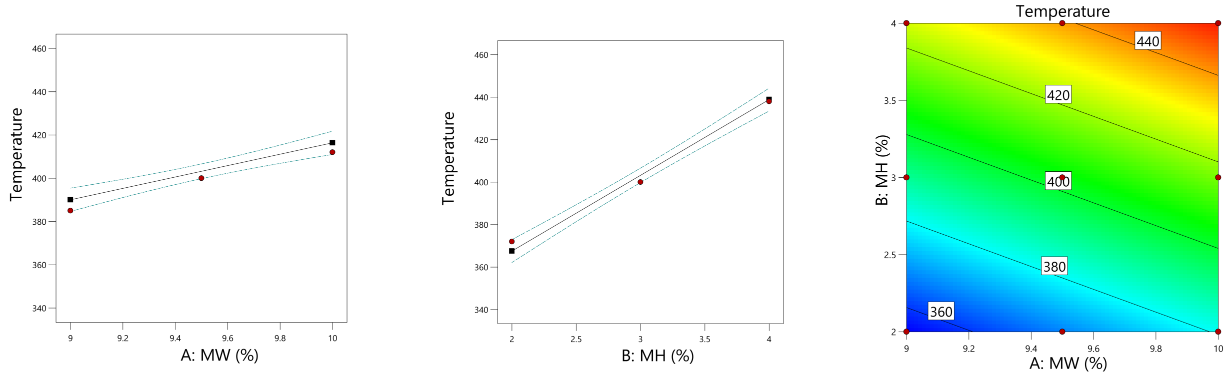

(a) (b) (c)

Fig. 7. Main effect plots and contour plots of the effects of M_w and M_h on drilling temperature.

3.42 Surface Plots of Force

Fig. 8 shows the surface and contour plots for drilling force with respect to M_w and M_h. The response surface plot for thrust force shows that both M_w and M_h contribute to increased force, but the effect of M_h is more significant (**Fig. 8**a). The surface shows a gradual rise along the M_w axis and a steeper increase along the M_h axis. This behavior can be attributed to increased interference between the drill margin and the workpiece as the margin height increases, resulting in greater resistance to tool penetration. The contour plot indicates a slightly curved pattern and a nonlinear relationship with Mh (**Fig. 8**b). The interaction effect between M_w and M_h was weak, as the surface shows little twisting. This observation aligns with the ANOVA results, where the interaction term (AB) was found to be marginally insignificant (p-value = 0.0582).

At a constant margin width of M_w = 9%, the thrust force increased from 820 N to 1080 N when the margin height increased from 2% to 4%. This increase can be attributed to the greater normal contact force generated between the drill margin and the hole wall. As the margin height increases, radial interference between the tool and the workpiece increases, resulting in greater frictional resistance during drilling. Whereas, at M_h = 3%, increasing the margin width from 9% to 10% increased the thrust force from 880 N to 960 N. Although this increase is noticeable, it is smaller than the effect produced by changes in margin height. This trend indicates that M_h plays a more dominant role in determining the magnitude of thrust force during drilling.

The interaction between the two parameters is also evident in the results. At larger margin heights, the increase in margin width further amplifies the thrust force due to the combined effect of increased contact area and friction. Such interaction effects are important in determining the optimal geometry of drill margins.

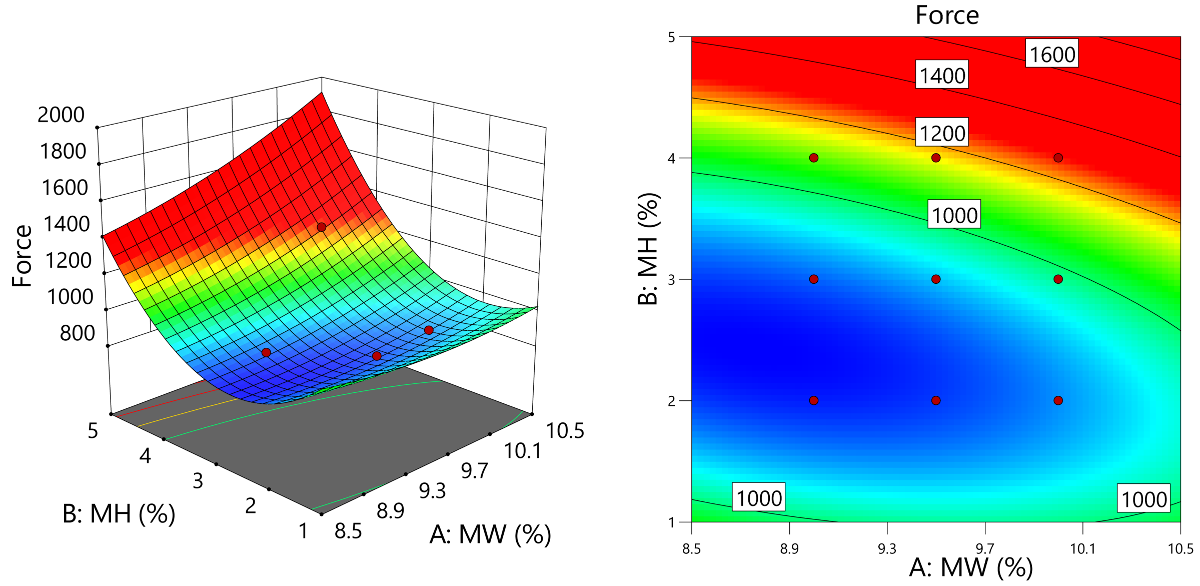

(a) (b)

Fig. 8. Surface and contour plots for drilling force.

3.43 Surface Plots of Torque

Fig. 9 shows the surface and contour plots for drilling torque. The response surface for torque shows a strong dependence on both M_w and M_h, with a dominant influence of M_h (Fig. 9a). The surface shows a steep increase in torque with increasing M_h, while M_w contributes to a lesser extent but remains significant. The contour plot reveals nearly parallel contour lines with slight curvature, indicating that the interaction between M_w and M_h is not significant (Fig. 9b). This confirms that the parameters primarily affect torque independently. Additionally, the curvature observed along the M_w direction suggests a nonlinear effect, consistent with the ANOVA results, which found the quadratic term of M_w to be insignificant (p-value = 0.4228).

The torque values obtained from the simulations ranged from 4700 N·mm to 5450 N·mm. The observed trends show that torque generally increases with both margin width and margin height. At M_w = 9%, increasing the margin height from 2% to 4% caused the torque to increase from 4700 N·mm to 5200 N·mm. This behavior is consistent with the increase in thrust force and frictional interaction at higher margin heights. Larger frictional resistance along the hole wall results in a greater rotational load on the drill, which increases the torque required for drilling.

A similar trend is observed for variations in margin width. At M_h = 3%, increasing the margin width from 9% to 10% resulted in an increase in torque from 4950 N·mm to 5150 N·mm. The wider margin increases the rubbing contact area and therefore contributes to higher frictional resistance during tool rotation.

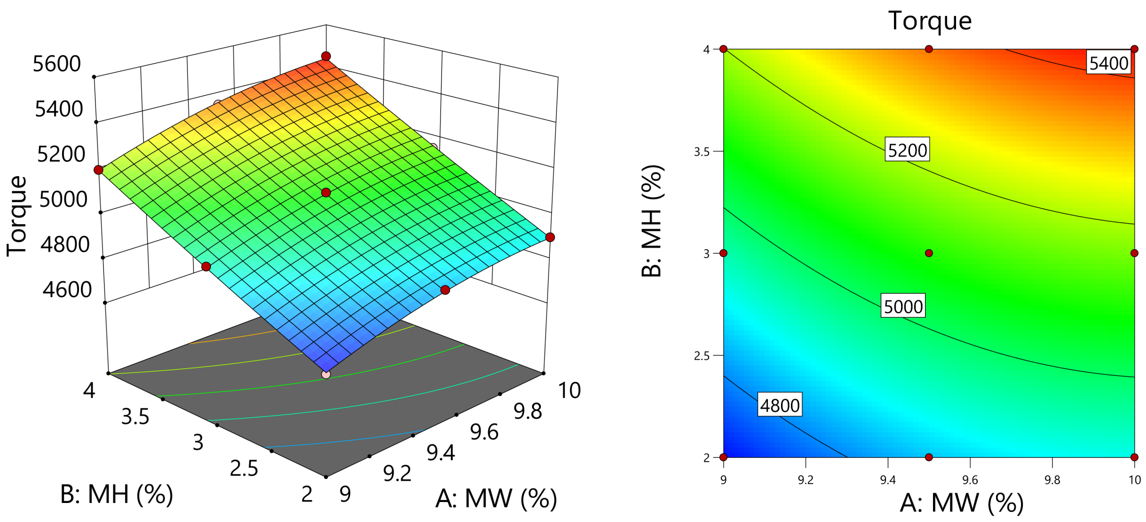

(a) (b)

Fig**9** . Surface and contour plots for drilling torque

3.44 Key Findings in Surface Plots Analysis

Overall, the response surface analysis reveals that margin height is the most influential parameter affecting all three responses (temperature, thrust force, and torque). The reason is primarily due to its direct role in controlling the radial contact and frictional interaction between the drill margin and the hole wall. Increasing M_h increases effective interference and normal stress at the margin-hole interface, thereby amplifying frictional shear stress (**Fig. 10**a). This stress results in increased energy dissipation as heat, as well as higher resistance to tool penetration and rotation. This phenomenon could elevate temperature, thrust force, and torque. Margin width plays a secondary role by influencing the contact area rather than the contact intensity (**Fig. 10**b). The interaction between M_w and M_h is generally weak, indicating that their effects on drilling performance are largely independent.

The combined results from the response surface plots and ANOVA analysis indicate that increasing margin dimensions result in higher thermal and mechanical loads during drilling. Therefore, minimizing both M_w and M_h within practical limits is essential for improving drilling performance. The consistency between the response surface trends and the ANOVA results' statistical significance confirms the robustness of the developed model and provides strong confidence in the optimization results.

The simulation results indicate that the interaction between margin width and margin height plays an important role in determining drilling performance. When both parameters increase simultaneously, the combined increase in contact area between the drill margin and the hole wall leads to significant increases in temperature, thrust force, and torque. The highest temperature (455 °C), thrust force (1280 N), and torque (5450 N·mm) were observed at the largest margin configuration of M_w = 10% and M_h = 4%. These results unveiled that excessive margin dimensions can lead to substantial frictional loading during drilling. Conversely, the lowest thermal and mechanical loads were observed at M_w = 9% and M_h = 2%, where the temperature, thrust force, and torque were 355 °C, 820 N, and 4700 N·mm, respectively. Smaller margin dimensions reduce the contact area between the drill and the hole wall, thereby minimizing frictional interaction and heat generation. These results highlight the importance of carefully balancing margin dimensions to achieve stable drilling while minimizing friction-induced thermal and mechanical loads.

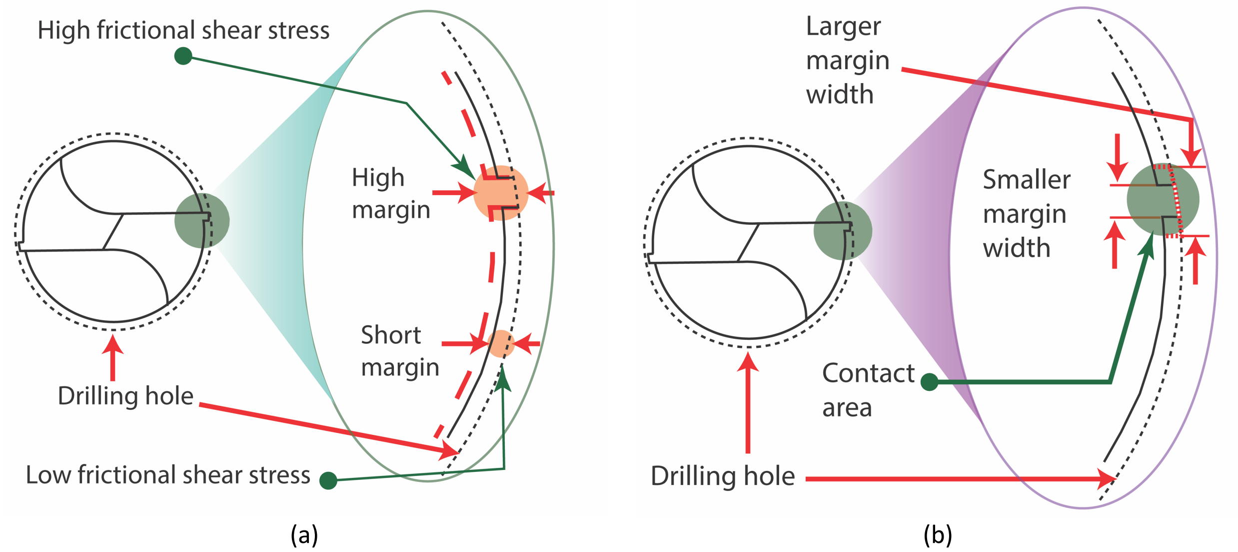

Fig. 10. Influence of margin height and width size on the (a) frictional shear stress and (b) contact area in drilling of Ti-6Al-4V

3.5 Desirability Analysis and Confirmation Tests

Multi-response optimization was performed using the desirability function approach, with M_w constrained within 9–10 %, M_h within 2–4 %, and all three responses (T_{max} range = 355–455°C, thrust force range = 820–1280 N, and torque range = 4700–5450 Nmm) are set to minimize (

Table 7). Equal weighting was applied to both margin parameters, while the three thermal and mechanical responses were assigned higher importance to prioritize drilling performance over geometric flexibility.

The optimization yielded a desirability value of 0.986 (**Table 8**), indicating that the identified margin configuration simultaneously minimizes temperature, thrust force, and torque to a degree very close to the theoretical optimum. Three confirmation runs validated the RSM predictions against FEM results, with errors of 0.00–2.28% for T_{max}, 0.38–2.58% for thrust force, and 0.37–2.61% for torque. These errors are all within the 95% prediction interval and therefore confirm the model accuracy across all responses.

The present study employed a coupled FEM–RSM framework because it enables both physical interpretation of drilling behavior and statistical quantification of parameter effects. Unlike black-box optimization methods, RSM provides explicit regression equations and ANOVA-based significance testing, which facilitate the interpretation of the influence of margin geometry on thermomechanical responses. Nevertheless, no direct comparison was performed with alternative optimization approaches such as Taguchi methods, genetic algorithms, particle swarm optimization, or machine-learning-based models. These techniques may offer advantages in exploring larger design spaces or identifying global optima. Therefore, future research should benchmark the FEM–RSM framework against advanced optimization algorithms in terms of prediction accuracy, computational efficiency, and optimization capability.

Table 7
Constraints for multi-objective optimization using desirability analysis.

Name	Goal	Lower Limit	Upper Limit	Lower Weight	Upper Weight	Importance
A:M_w	is in range	9	10	1	1	3
B:M_h	is in range	2	4	1	1	3
Temperature	minimize	355	455	1	1	5
Force	minimize	820	1280	1	1	5
Torque	minimize	4700	5450	1	1	5

Table 8
Optimal solutions from the multi-objective optimization

Number	MW	MH	Temperature	Force	Torque	Desirability
1	9.000	2.000	354.389	835.278	4706.944	0.986
2	9.000	2.010	354.737	834.580	4709.182	0.985
3	9.000	2.019	355.076	833.918	4711.363	0.985

Table 9
Confirmation tests between predicted and actual thermomechanical response in Ti-6Al-4V drilling.

Solution no.	M_w (%)	M_h (%)	Actual	Predicted	Residual	Error (%)
			T_{max} (°C)			
			355.3	354.4	-0.9	0.25
			Force (N)			
1	9.000	2.000	820.4	835.3	-14.9	1.82
			Torque (Nmm)			
			4698.8	4706.9	-8.1	0.17

3.6 Limitations of Current Study

Although the developed FEM–RSM framework demonstrated good predictive capability for evaluating the influence of drill margin geometry, several limitations should be acknowledged. First, the drill was modeled as a rigid body, and progressive tool wear was not considered. In practical drilling operations, tool wear alters the cutting-edge geometry and frictional conditions, potentially altering temperature generation, thrust force, and torque during prolonged machining.

Second, the simulations assumed stable continuous cutting conditions and did not account for intermittent phenomena such as chatter vibrations, tool runout, chip adhesion, or transient chip breakage. These effects may influence the local contact conditions and thermomechanical responses observed during actual drilling operations.

Third, the numerical model was validated using available thrust force and torque measurements reported in the literature. Experimental temperature measurements for the selected validation conditions were unavailable; therefore, direct validation of the predicted temperatures was not possible. Consequently, the thermal predictions should be interpreted within the assumptions and limitations of the numerical model.

Finally, the present study focused exclusively on dry drilling conditions and investigated only two margin parameters (M_w and M_h), while other geometric features and cooling strategies were maintained constant. Future studies should incorporate tool wear evolution, experimental validation of temperature, advanced friction formulations, and coolant-assisted drilling conditions to improve model fidelity and industrial applicability further.

4. Conclusions

This study investigated the influence of drill margin geometry on drilling performance during titanium alloy machining using a finite-element modelling approach combined with response surface methodology. Based on the simulation results and statistical analysis, the following conclusions can be drawn:

- The developed thermo-mechanical finite element model successfully predicted the drilling responses, including temperature, thrust force, and torque. Validation against experimental results reported in Simulation modeling of drilling performance using FEM and RSM showed good agreement, with an average prediction error of approximately 2.5% for thrust force and less than 8% for torque.
- Both margin width (M_w) and margin height (M_h) significantly influence drilling performance by affecting the contact between the drill margin and the hole wall. Increasing either parameter increases frictional contact, resulting in higher drilling temperature, thrust force, and torque.
- Margin height was identified as the dominant parameter affecting thrust force and torque, while margin width exhibited a secondary but noticeable influence on the thermal and mechanical responses of the drilling process.
- Response surface analysis indicated that both margin width and margin height contribute to increased temperature, thrust force, and torque. The interaction between M_w and M_h was generally weak. For thrust force, the interaction term was marginally significant ($p = 0.0582$), suggesting a limited synergistic effect when both parameters increased simultaneously. In contrast, the interaction effect on torque was statistically insignificant ($p = 0.1443$), indicating that the influence of M_w and M_h was predominantly independent. Overall, margin height was identified as the dominant factor governing the thermomechanical responses during drilling. Excessively large margin dimensions can therefore negatively affect drilling performance.
- The optimal drilling performance within the investigated design space was achieved at M_w = 9% and M_h = 2%, resulting in the lowest temperature, thrust force, and torque. This configuration minimizes frictional interaction while maintaining adequate drill guidance.

Overall, the developed FEM–RSM framework provides an effective approach for evaluating drill geometry and optimizing tool design parameters to improve drilling performance in titanium alloys.

Acknowledgement
This research was supported by the Ministry of Higher Education (MOHE) Malaysia through the Fundamental Research Grant Scheme (FRGS/1/2023/TK10/UMT/02/1).

References

[1] Subrahmanyam, A.P.S.V.R, Kondapalli Siva Prasad, and P.Srinivasa Rao. 2020. A Review on Mechanical and Corrosion Behaviour of DMLS Materials. *Engineering Science & Technology* 1: 62–83. https://doi.org/10.37256/est.122020319.

[2] Zhai, Chuanmiao, Xubo Li, Cunqiang Zang, Shihao Zhang, Bian Guo, Canjun Wang, Xiaolong Gao, Yuewen Su, and Mengmeng Liu. 2025. Modeling and Experimental Investigation of Ultrasonic Vibration-Assisted Drilling Force for Titanium Alloy. *Materials* 18: 4460. https://doi.org/10.3390/ma18194460.

[3] Mathiyazhagan, Vijayathithan, and Anil Meena. 2025. A new approach for analyzing machining-induced damage in correlation with tool wear during dry drilling of CFRP/Ti stacks. *Proceedings of the Institution of Mechanical Engineers, Part B: Journal of Engineering Manufacture* 239: 851–876. https://doi.org/10.1177/09544054241249780.

[4] Dai, Nianwei, Lai-Chang Zhang, Junxi Zhang, Xin Zhang, Qingzhao Ni, Yang Chen, Maoliang Wu, and Chao Yang. 2016. Distinction in corrosion resistance of selective laser melted Ti-6Al-4V alloy on different planes. *Corrosion Science* 111: 703–710. https://doi.org/10.1016/j.corsci.2016.06.009.

[5] Dalke, Piyush A, Atul Vasant Karanjkar, and Pankaj Wankhede. 2024. Multi response optimization of process parameters in titanium alloy minimum quantity lubrication drilling operation. *Engineering Research Express* 6: 045412. https://doi.org/10.1088/2631-8695/ad7cc7.

[6] Le Coz, G., M Jrad, Pascal Laheurte, and D Dudzinski. 2017. Analysis of local cutting edge geometry on temperature distribution and surface integrity when dry drilling of aeronautical alloys. *The International Journal of Advanced Manufacturing Technology* 93: 2037–2044. https://doi.org/10.1007/s00170-017-0671-9.

[7] Mughal, Kiran, Mohammad Pervez Mughal, Muhammad Umar Farooq, Muhammad Qaiser Saleem, and Rodolfo Haber Guerra. 2023. Helical Milling of CFRP/Ti6Al4V Stacks Using Nano Fluid Based Minimum Quantity Lubrication (NF-MQL): Investigations on Process Performance and Hole Integrity. *Materials* 16: 566. https://doi.org/10.3390/ma16020566.

[8] Shareef, Israa R, Hiba K Hussein, and Basma L Mahdi. 2023. Experimental Investigation and Fuzzy Based Prediction of Titanium Alloy Performance During Drilling Process. *Advances in Science and Technology Research Journal* 17. Society of Polish Mechanical Engineers and Technicians: 192–205. https://doi.org/10.12913/22998624/174515.

[9] Akhbar, Mohd Faizal Ali, Shahrizan Jamaludin, Suriani Mat Jusoh, Fatin Alias, Mohd Azlan Musa, and Rodianah Alias. 2026. Thermal performance of modified surgical drill margins during bone drilling: An experimental, numerical, and optimization case study. *Proceedings of the Institution of Mechanical Engineers, Part H: Journal of Engineering in Medicine*. IMECHE: 09544119261426440. https://doi.org/10.1177/09544119261426440.

[10] Akhbar, Mohd Faizal Ali. 2023. Thermomechanical damage in cortical bone caused by margins of surgical drill bit: A finite element analysis. *Computer Methods and Programs in Biomedicine* 231. Elsevier B.V.: 107361. https://doi.org/10.1016/j.cmpb.2023.107361.

[11] Akhbar, Mohd Faizal Ali, and Akmal Wani Sulong. 2021. Surgical drill bit design and thermomechanical damage in bone drilling: a review. *Annals of Biomedical Engineering* 49. Springer International Publishing: 29–56. https://doi.org/10.1007/s10439-020-02600-2.

[12] Samsudeensadham, S, V Krishnaraj, and ArunRamnath Ramachandran. 2025. Multi-attribute optimization of drilling CFRP/Ti-6Al-4V alloy hybrid stacks using VIKOR. *Proceedings of the Institution of Mechanical Engineers, Part E: Journal of Process Mechanical Engineering* 239: 2556–2569. https://doi.org/10.1177/09544089231206037.

[13] Roldán-Jiménez, Luis, Severo Raúl Fernández-Vidal, Francisco Javier Puerta-Morales, Ana Pilar Valerga-Puerta, and Fermín Bañón-García. 2023. Design and Evaluation of an Eco-Efficient RHVT-Cooled Ti6Al4V Drilling Process. *Key Engineering Materials* 955: 63–71. https://doi.org/10.4028/p-9lUdKL.

[14] Ali Akhbar, Mohd Faizal, and Ahmad Razlan Yusoff. 2019. Drilling of bone: Effect of drill bit geometries on thermal osteonecrosis risk regions. *Proceedings of the Institution of Mechanical Engineers. Part H, Journal of engineering in medicine* 233: 207–218. https://doi.org/10.1177/0954411918819113.

[15] Akhbar, Mohd Faizal Ali, and Ahmad Razlan Yusoff. 2019. Multi-objective optimization of surgical drill bit to minimize thermal damage in bone-drilling. *Applied Thermal Engineering* 157. Elsevier: 113594. https://doi.org/10.1016/j.applthermaleng.2019.04.004.

[16] Singh, Narender, and Pushpendra S Bharti. 2022. Experimental investigations and parametric optimization during micro-EDM drilling of Ti -5.6Al-3.6V using ABC algorithm. *Journal of Engineering Research*. https://doi.org/10.36909/jer.ICMET.17201.

[17] Chatterjee, Suman, Siba Sankar Mahapatra, and Kumar Abhishek. 2016. Simulation and optimization of machining parameters in drilling of titanium alloys. *Simulation Modelling Practice and Theory* 62. Elsevier B.V.: 31–48. https://doi.org/10.1016/j.simpat.2015.12.004.

[18] Ali Akhbar, Mohd Faizal, and Ahmad Razlan Yusoff. 2019. Comparison of bone temperature elevation in drilling of human, bovine and porcine bone. *Procedia CIRP* 82. Elsevier B.V.: 411–414. https://doi.org/10.1016/j.procir.2019.03.220.

[19] Akhbar, Mohd Faizal Ali, and Ahmad Razlan Yusoff. 2020. Fast & Injurious: Reducing thermal osteonecrosis regions in the drilling of human bone with multi-objective optimization. *Measurement* 152: 107385. https://doi.org/10.1016/j.measurement.2019.107385.

[20] Akhbar, Mohd Faizal Ali, Shahrizan Jamaludin, Razhan Hassan, and Akmal Wani Sulong. 2024. Drilling of Bone: Effect of Drill Bit Clearance on Thermal Damage. In *Advanced Structured Materials*, 215:207–214. https://doi.org/10.1007/978-3-031-64330-9_18.

[21] Ali Akhbar, Mohd Faizal, Mohamad Faris Mohd Ashri, Ahmad Razlan Yusoff, Shahrizan Jamaludin, Rodianah Alias, Fatin Alias, Razhan Hassan, and Muhammad Rizwan. 2024. Optimization of Drill Bit Geometries for Minimum Thermal Damage in Bone Drilling. *Journal of Advanced Research in Fluid Mechanics and Thermal Sciences* 122: 22–37. https://doi.org/10.37934/arfmts.122.2.2237.